

TECHNICAL ADVANCE

A multicolored set of *in vivo* organelle markers for co-localization studies in *Arabidopsis* and other plants

Brook K. Nelson[†], Xue Cai^{†,‡} and Andreas Nebenführ^{*}

Department of Biochemistry, Cellular and Molecular Biology, University of Tennessee, Knoxville, TN 37996-0840, USA

Received 13 February 2007; revised 25 May 2007; accepted 4 June 2007.

^{*}For correspondence: (fax +1 865 974 6306; e-mail nebenfuehr@utk.edu).[†]These authors contributed equally to this work.[‡]Present address: Department of Cell Biology, University of Oklahoma Health Sciences Center, Oklahoma City, OK, USA.

Summary

Genome sequencing has resulted in the identification of a large number of uncharacterized genes with unknown functions. It is widely recognized that determination of the intracellular localization of the encoded proteins may aid in identifying their functions. To facilitate these localization experiments, we have generated a series of fluorescent organelle markers based on well-established targeting sequences that can be used for co-localization studies. In particular, this organelle marker set contains indicators for the endoplasmic reticulum, the Golgi apparatus, the tonoplast, peroxisomes, mitochondria, plastids and the plasma membrane. All markers were generated with four different fluorescent proteins (FP) (green, cyan, yellow or red FPs) in two different binary plasmids for kanamycin or glufosinate selection, respectively, to allow for flexible combinations. The labeled organelles displayed characteristic morphologies consistent with previous descriptions that could be used for their positive identification. Determination of the intracellular distribution of three previously uncharacterized proteins demonstrated the usefulness of the markers in testing predicted subcellular localizations. This organelle marker set should be a valuable resource for the plant community for such co-localization studies. In addition, the *Arabidopsis* organelle marker lines can also be employed in plant cell biology teaching labs to demonstrate the distribution and dynamics of these organelles.

Keywords: organelles, fluorescent protein, protein localization, *Arabidopsis thaliana*.

Introduction

Cells are highly complex systems that carry out a large number of biochemical functions. To allow for efficient concurrent execution of these functions, cells of eukaryotic organisms such as plants are organized into a large number of compartments, the membrane-bound organelles, which specialize in different metabolic processes. For example, photosynthesis occurs in chloroplasts whereas cellular respiration takes place in mitochondria. The biochemical capabilities of an organelle are largely defined by the proteins/enzymes present in this compartment. This fact has been used for many years in the form of marker enzymes for cell fractionation studies (Lunn, 2006). On the other hand, the intracellular localization of an uncharacterized protein can be used to infer the likely functions of this protein. This concept has led to the development of several

computational and experimental approaches for determining the subcellular localization of proteins (Lunn, 2006).

Computational approaches to predict protein localization typically take advantage of short sequence motifs that act like postal codes, and are recognized by specific proteins that mediate the import of the protein into an organelle. For example, the signal sequence at the N-terminus of newly synthesized proteins is recognized by the signal recognition particle, which then directs synthesis of the remainder of the protein to the endoplasmic reticulum (ER) for co-translational insertion into the secretory pathway (Vitale and Denecke, 1999). Other targeting motifs are found at the C-terminus of proteins, such as the ER retention signal (His/Lys-Asp-Glu-Leu; see e.g. Crofts *et al.*, 1999), or somewhere in the middle of the protein (e.g. Vitale and Raikhel, 1999).

A number of protein targeting motifs have been identified in the past, which has led to the creation of several computer programs that attempt to predict the subcellular localization of a protein based on its amino acid (aa) sequence. However, many targeting motifs are only poorly defined and seem to allow for a substantial variation in aa sequences (Emanuelsson and von Heijne, 2001). Combined with potential additional, currently unknown targeting motifs, this makes accurate targeting predictions difficult (Li *et al.*, 2006).

Experimental approaches to determine protein localization rely on either biochemical purification of organelles or direct visualization of subcellular distribution. In the former case, the advent of organelle proteomics has allowed researchers to identify a large number of proteins associated with an organelle (Komatsu *et al.*, 2006). Organelle proteomics has the advantage that it is unbiased, i.e. does not depend on previous knowledge of protein composition. However, potential problems are that minor constituents could be missed and that unexpected protein identifications could result from contamination with other cellular constituents (Dunkley *et al.*, 2006; Lilley and Dupree, 2006). In addition, organelle proteomics is not an efficient approach when the localization of a specific candidate is to be identified.

Localization of a protein of interest within a cell, on the other hand, overcomes this problem by directly visualizing its distribution. Ideally, this localization is based on immunohistochemistry with specific antibodies that recognize the native conformation of the protein. This approach reveals the subcellular localization of the native protein under normal expression conditions, and can therefore be considered the 'gold standard' for this kind of question. However, generation of the specific antibody is both time consuming and expensive, and may not always be successful, as in the case of closely related gene family members. Alternatively, fusions of protein-coding regions to genes of fluorescent proteins (FPs) allow for a simple and often sufficient approach to identify subcellular distribution in living cells (Dixit *et al.*, 2006). FP fusions also have the potential of being scaled up for high-throughput screens (Cutler *et al.*, 2000; Escobar *et al.*, 2003; Koroleva *et al.*, 2005; Tian *et al.*, 2004). Although the fluorescence pattern can sometimes be identified as similar to a specific organelle, it is often necessary to compare the distribution of the uncharacterized protein to well-established organelle markers in the same cell.

A large number of fluorescent organelle markers have been developed over the years (Dhanoo *et al.*, 2006); however, they exist in a variety of vector systems and must be requested from different sources. In addition, many of the markers are based solely on GFP, thus limiting the options for multilabeling experiments. To overcome these problems we have generated a unified collection of fluorescent markers for several membrane-bounded organelles in plant cells. All markers were made with four different FPs (CFP,

GFP, YFP and mCherry) and in two different binary vectors (pBIN and pFGC) to facilitate the free combination of these markers with each other and with other constructs. In this report we describe characteristic features of these organelle markers, and demonstrate their usefulness for the identification of localization of uncharacterized proteins.

Results and discussion

Organelle markers are based on well-established targeting sequences

The organelle markers in this set are based on targeted localization of FPs to specific subcellular compartments. The localization information for most constructs was provided by well-established short targeting signals, so that the markers did not introduce any new enzymatic activity that might alter cellular behavior. Despite this attempt to provide minimal interference with cellular function, it is possible that the mere presence of an overexpressed marker protein may disrupt, for example, the transport of normal residents of these organelles. However, we have not observed any obvious deleterious effects of the marker proteins on plant growth and development after several generations.

The plastid marker was based on the targeting sequence (first 79 aa) of the small subunit of tobacco rubisco (Dabney-Smith *et al.*, 1999), whereas mitochondrial targeting was achieved by incorporating the first 29 aa of yeast (*Saccharomyces cerevisiae*) cytochrome *c* oxidase IV (ScCOX4; Köhler *et al.*, 1997). Fluorescent proteins were imported into peroxisomes after addition of the peroxisomal targeting signal 1 (PTS1, Ser-Lys-Leu) at their C-termini (Reumann, 2004). Golgi localization was based on the cytoplasmic tail and transmembrane domain (first 49 aa) of GmMan1, soybean α -1,2-mannosidase I (Saint-Jore-Dupas *et al.*, 2006). The ER marker was created by combining the signal peptide of AtWAK2 (*Arabidopsis thaliana* wall-associated kinase 2; He *et al.*, 1999) at the N-terminus of the FP and the ER retention signal His-Asp-Glu-Leu at its C-terminus (Gomord *et al.*, 1997).

The only exceptions from the use of well-defined short targeting signals were the tonoplast and plasma membrane markers, which were based instead on fusions to full-length proteins. In particular, tonoplast localization was achieved by fusing the coding region of the FP to the C-terminus of γ -TIP, an aquaporin of the vacuolar membrane (Saito *et al.*, 2002). This approach was necessary as targeting signals for tonoplast proteins have not been established, and soluble FPs in the lumen of vacuoles often lack fluorescence signals because of the low pH of the vacuole (Tamura *et al.*, 2003). It should be noted that γ -TIP may not label all vacuolar membranes (Jauh *et al.*, 1999); however, it provides an excellent marker for the tonoplast surrounding the large central vacuole of mature plant cells. Plasma membrane

Table 1 Organelle markers available as binary plasmids and in Arabidopsis (Col)

Organelle	Binary plasmids				Plants		
	<i>CFP</i>	<i>GFP</i>	<i>YFP</i>	<i>mCherry</i>	<i>CFP</i>	<i>GFP</i>	<i>YFP</i>
ER	ER-ck <i>CD3-953</i> ER-cb <i>CD3-954</i>	ER-gk <i>CD3-955</i> ER-gb <i>CD3-956</i>	ER-yk <i>CD3-957</i> ER-yb <i>CD3-958</i>	ER-rk <i>CD3-959</i> ER-rb <i>CD3-960</i>	ER-ck <i>CS16250</i>	ER-gk <i>CS16251</i>	ER-yk <i>CS16252</i>
Golgi	G-ck <i>CD3-961</i> G-cb <i>CD3-962</i>	G-gk <i>CD3-963</i> G-gb <i>CD3-964</i>	G-yk <i>CD3-965</i> G-yb <i>CD3-966</i>	G-rk <i>CD3-967</i> G-rb <i>CD3-968</i>	G-ck <i>CS16253</i>	G-gk <i>CS16254</i>	G-yk <i>CS16255</i>
tonoplast	vac-ck <i>CD3-969</i> vac-cb <i>CD3-970</i>	vac-gk <i>CD3-971</i> vac-gb <i>CD3-972</i>	vac-yk <i>CD3-973</i> vac-yb <i>CD3-974</i>	vac-rk <i>CD3-975</i> vac-rb <i>CD3-976</i>	vac-ck <i>CS16256</i>	vac-gk <i>CS16257</i>	vac-yk <i>CS16258</i>
peroxisomes	px-ck <i>CD3-977</i> px-cb <i>CD3-978</i>	px-gk <i>CD3-979</i> px-gb <i>CD3-980</i>	px-yk <i>CD3-981</i> px-yb <i>CD3-982</i>	px-rk <i>CD3-983</i> px-rb <i>CD3-984</i>	px-ck <i>CS16259</i>	px-gk <i>CS16260</i>	px-yk <i>CS16261</i>
mitochondria	mt-ck <i>CD3-985</i> mt-cb <i>CD3-986</i>	mt-gk <i>CD3-987</i> mt-gb <i>CD3-988</i>	mt-yk <i>CD3-989</i> mt-yb <i>CD3-990</i>	mt-rk <i>CD3-991</i> mt-rb <i>CD3-992</i>	mt-ck <i>CS16262</i>	mt-gk <i>CS16263</i>	mt-yk <i>CS16264</i>
plastids	pt-ck <i>CD3-993</i> pt-cb <i>CD3-994</i>	pt-gk <i>CD3-995</i> pt-gb <i>CD3-996</i>	pt-yk <i>CD3-997</i> pt-yb <i>CD3-998</i>	pt-rk <i>CD3-999</i> pt-rb <i>CD3-1000</i>	pt-ck <i>CS16265</i>	pt-gk <i>CS16266</i>	pt-yk <i>CS16267</i>
plasma membrane	pm-ck <i>CD3-1001</i> pm-cb <i>CD3-1002</i>	pm-gk <i>CD3-1003</i> pm-gb <i>CD3-1004</i>	pm-yk <i>CD3-1005</i> pm-yb <i>CD3-1006</i>	pm-rk <i>CD3-1007</i> pm-rb <i>CD3-1008</i>			

Nomenclature of markers: abbreviations to the left of hyphens indicate the targeted organelle; the color of the construct and selection in plants is indicated on the right; c, CFP; g, GFP; y, YFP; r, mCherry; k, kanamycin selection; b, basta (glufosinate) selection. Italicized numbers (*CD3-xxx* or *CS162xx*) indicate ABRC stock numbers (<http://www.arabidopsis.org>).

labeling was based on the full-length coding region of *AtPIP2A*, a plasma membrane aquaporin (Cutler *et al.*, 2000).

All markers were generated with four different FPs, GFP, CFP, YFP and mCherry (a red FP; Shaner *et al.*, 2004) to provide flexibility for different co-localization experiments (Table 1). For example, the CFP-based markers could be used in combination with YFP-labeled proteins to test localization of the unknown protein to a specific organelle, or vice versa. GFP markers can be used in double-labeling experiments together with the red mCherry constructs or rhodamine-labeled antibodies. All markers employ the strong and nearly ubiquitously expressed 35S promoter with dual enhancer elements (d35S), with the exception of the green tonoplast markers that are driven by regular 35S promoters. The markers were constructed in two different binary expression vectors for *Agrobacterium tumefaciens*-mediated plant transformation, to allow for kanamycin or glufosinate (basta) selection, respectively (Table 1). Finally, the kanamycin-selection plasmids were used to create stable Arabidopsis lines with GFP-, CFP- or YFP-labeled organelles (Table 1). Both the binary plasmids and plant lines are made available through the Arabidopsis stock centers (<http://www.arabidopsis.org>).

Fluorescently labeled organelles can be identified by their characteristic morphologies

The labeled organelles included in this set are the ER, the Golgi apparatus, the tonoplast, peroxisomes, mitochondria, plastids and the plasma membrane. Other organelles, such as the endosomes or pre-vacuolar compartments, have been excluded from this collection as short targeting signals have not been identified for them. Furthermore, the

only known marker proteins for post-Golgi organelles are directly involved in trafficking to or from these organelles (e.g. Rab proteins, Molendijk *et al.*, 2004; SNAREs, Uemura *et al.*, 2004; or sorting receptors, Tse *et al.*, 2004), and may interfere with the normal functioning of the organelle. The nucleus was also not included in this set as its prominent size makes identification trivial. In the following text we describe some characteristic features of the FP-labeled organelles that can aid in their identification. All images presented in this report have been generated with conventional epifluorescence microscopy to illustrate the appearance of the organelles as seen through the eyepieces of a microscope. For an in-depth introduction to live-cell microscopy readers are referred to a recent tutorial (Shaw, 2006).

Organelles in eukaryotic cells can be grouped, based on their appearance in the microscope, into those that are predominantly small and round, and those that have a long, extended morphology. Organelles in the first group are typically present in many copies per cell, leading to a punctate pattern of the organelle marker. The extended organelles, on the other hand, are usually found as a single interconnected structure that stretches throughout the cytoplasm, leading to a tubular or sheet-like morphology. The appearance of the organelles, particularly in the second group, depends critically on the position of the focal plane within the cell. In most cases, visualization of the organelles in the plane of the cortical cytoplasm underlying the plasma membrane is most informative. All the organelles labeled with this set of markers with the exception of the plasma membrane show an actin-myosin-dependent movement in the cytoplasm (Boevink *et al.*, 1998; Collings *et al.*, 2002; van Gestel *et al.*, 2002; Jedd and Chua, 2002; Kwok and Hanson,

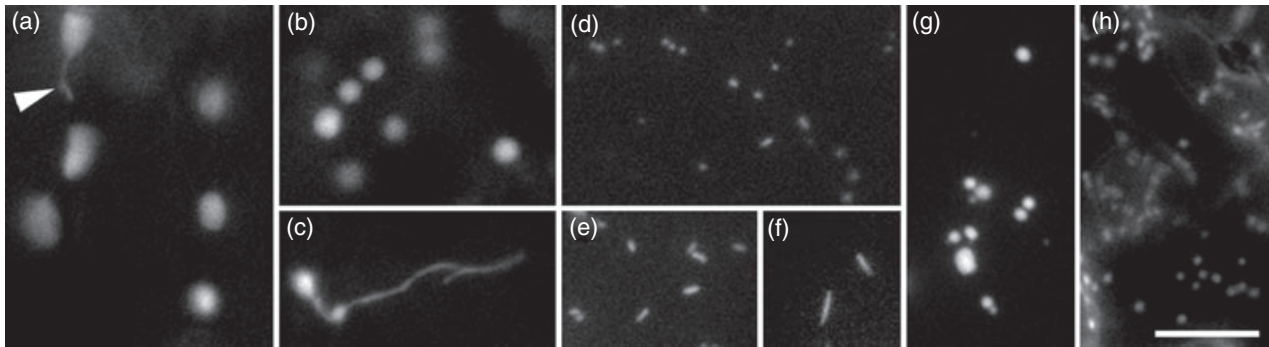


Figure 1. Typical morphology of punctate organelles in the cortical cytoplasm of *Arabidopsis* leaf epidermal cells, except where indicated. (a)–(c) Plastids. (a) Plastids in the left cell were slightly larger than those in the right cell. The arrowhead indicates a stromule on the upper left plastid. (b) Apparent differences in brightness between different plastids in the same cell caused by out-of-focus plastids. (c) Plastid in onion epidermal cell with a prominent stromule. (d)–(f) Mitochondria. (d) Typical appearance of mitochondria as numerous small spots. (e) Sometimes mitochondria were elongated and had the shape of rice grains. (f) Some cells contained relatively few mitochondria that were even longer. (g) Peroxisomes were typically round in appearance, but varied in size even within a single cell. (h) Golgi stacks were found throughout the cells as small, nearly round, spots. All images were captured with conventional epifluorescence. Scale bar = 10 μm .

2003; Mano *et al.*, 2002; Mathur *et al.*, 2002; Nebenführ *et al.*, 1999). This movement is most easily recognized for punctate organelles, but also occurs for the more extended organelles (Runions *et al.*, 2006; Ruthardt *et al.*, 2005).

Plastids are often the largest of the punctate organelles, ranging in size from 2–3 μm for proplastids (Figure 1a–c) to roughly 5 μm for fully developed chloroplasts. Whereas chloroplasts can be easily identified by their green color in bright-field microscopy and by their typical red chlorophyll fluorescence, other plastid forms can benefit from the organelle markers provided in this set. This is particularly relevant for epidermal cells that are usually targeted by particle bombardment or leaf infiltration, and are easily accessible to fluorescent microscopy. In the epidermis, plastids can vary in size from cell to cell, but within a cell they have a fairly uniform diameter (Figure 1a,b). A unique characteristic of plastids is the occasional presence of long tubular branches, known as stromules (Figure 1a,c). These stromules are extensions of the plastid envelope that are filled with stroma, and therefore contain the soluble plastid marker (Kwok and Hanson, 2004). Not all plastids possess stromules, but when present they can be used as an identifying characteristic.

Mitochondria are typically small (approximately 0.5 μm in diameter), round and are present in high copy numbers in every cell (Figure 1d). However, their morphology can vary dramatically as a result of the fusion and fission of these organelles (Logan, 2006). Some cells may contain mitochondria that are a few micrometers long (Figure 1e,f); others may take on a worm-like shape or appear as beads on a string (Logan, 2006). These different morphologies can be observed from one cell to the next, but within a given cell all mitochondria display similar morphology. In rare cases, thin tubular extensions, so-called matrixules, can be observed

that appear to be similar to the stromules of plastids (Logan, 2006).

Peroxisomes also are small, typically round, organelles (Muench and Mullen, 2003). However, unlike mitochondria and plastids, their size can vary within a single cell from <0.5 to 2 μm (Figure 1g). In photosynthetically active cells, peroxisomes are often found in association with chloroplasts (Oikawa *et al.*, 2003) where they participate in photorespiration. The number of peroxisomes varies from cell to cell.

The Golgi apparatus consists of a large number of small (<1 μm) independent stacks (Figure 1h). The individual Golgi stacks can appear as perfectly round discs, as short lines or in the shape of small rings, depending on orientation and status (Nebenführ *et al.*, 1999). The Golgi marker may also show weak ER labeling, resulting from the continuous recycling of Golgi resident proteins through the ER (Brandizzi *et al.*, 2002). The identity of the FP spots as Golgi can also be ascertained by treatment with brefeldin A (BFA), which leads to a fusion of Golgi and ER membranes and relocation of Golgi proteins into the ER (Nebenführ *et al.*, 2002; Ritzenthaler *et al.*, 2002; Saint-Jore *et al.*, 2002). However, some *trans*-Golgi proteins can also respond to BFA by forming large clusters in the perinuclear region, the so-called BFA compartments (Baldwin *et al.*, 2001; Satiat-Jeunemaitre *et al.*, 1996; Wee *et al.*, 1998).

The ER forms, as the name indicates, an extensive network throughout the cytoplasm. This network is best observed by focusing on the cortical cytoplasm just under the plasma membrane (Figure 2a). In this case, a fine network of clearly delineated tubular and sheet-like ER elements can be discerned. The signal difference between the dark areas in the lacunae and the ER elements is substantial and distinct. By contrast, cytoplasmic FPs would

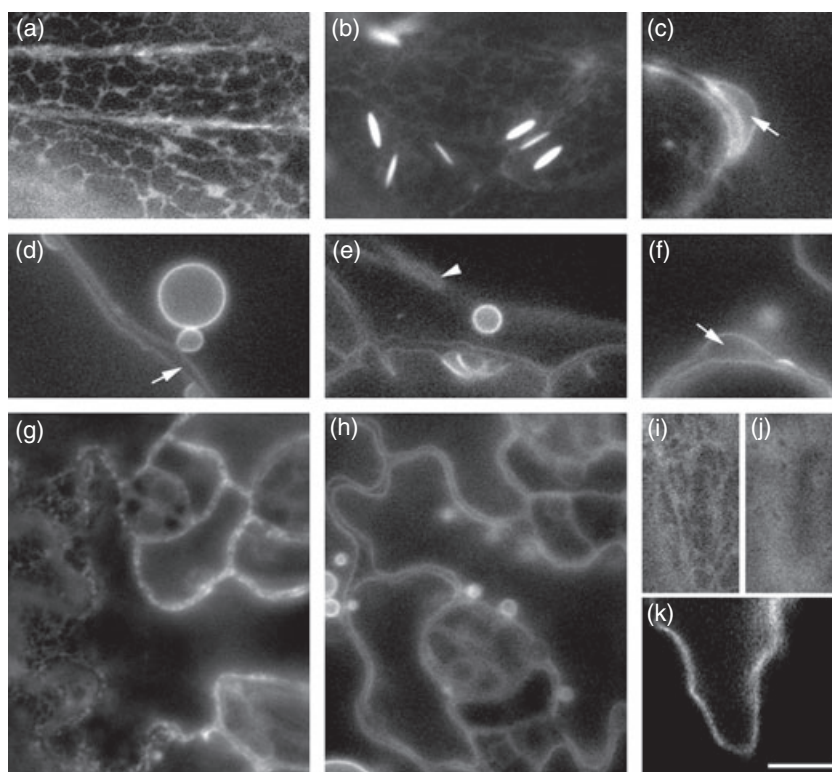


Figure 2. Characteristic features of extended organelles in leaf epidermal cells of *Arabidopsis*, except where indicated.

(a)–(c), (g) and (i) endoplasmic reticulum (ER). (d)–(f) and (h) Tonoplast. (j) Cytoplasmic fluorescent proteins (FP). (k) Plasma membrane.

(a) Cortical ER network showing sheet-like regions that are connected by tubular elements.

(b) Some cells may contain large, very bright, fusiform bodies that are local extensions of the ER.

(c) The ER is continuous with the nuclear envelope and surrounds the nucleus (arrow) on all sides.

(d) The tonoplast of seedlings may form circular extensions, 'bulbs', into the lumen of the vacuole. The arrow denotes the cell-wall space between two neighboring cells.

(e) Transvacuolar strands (arrowhead) are tonoplast-delimited cytoplasmic tunnels that seem to bisect the vacuole.

(f) The tonoplast is found only on one side of the nucleus (arrow), and not on the side facing the plasma membrane. (g) Overview of ER labeling in several cells. Note the stippled appearance of the ER seen in cross section in the right half of the image. The left half shows the cortical ER network of the cells in face-on view.

(h) Overview of tonoplast labeling in several cells. Note the clear separation of the tonoplasts from two neighboring cells and the uniform labeling along the edge of the vacuoles.

(i) Cortical ER in an onion epidermal cell. Note the distinct edge between ER elements and cytoplasmic regions ('lacunae').

(j) Cytoplasmic FP in the same cell as (i). Note the broad and diffuse staining that results from differences in the thickness of the cytoplasm. Small dark spots result from negative staining of unlabeled organelles.

(k) Plasma membrane labeling of a single cell in an *Arabidopsis* seedling 72 h after particle bombardment. Note the uniform labeling along the cell surface and the absence of discernible structures in the interior of the cell. Scale bar = 10 μm .

be seen as diffuse fluorescence (Figure 2, compare i and j). Some cell types, particularly in the seedling epidermis, also contain bright, elongated structures known as fusiform bodies or ER bodies (Figure 2b). These fusiform bodies are about 5 μm in length and 1- μm wide, and are local extensions of the ER that contain vegetative storage proteins (Hawes *et al.*, 2001). Formation of fusiform bodies can be induced by wounding, and depends on methyl jasmonate signaling (Matsushima *et al.*, 2003).

When fully expanded cells are viewed in a medial plane, the ER is seen only in the thin layer of cytoplasm underneath the plasma membrane and surrounding the nucleus (Figure 2g). The cortical ER often takes on a stippled appearance resulting from its network character. The perinuclear label-

ing, however, is more uniform because the ER is continuous with the nuclear envelope (Figure 2c). The ER marker can therefore also reveal the dynamic morphology of the nucleus (Collings *et al.*, 2000).

The tonoplast is the delimiting membrane around the vacuole, and in fully expanded cells stretches throughout the cell revealing the large size of the central vacuole (Figure 2h). Occasional transvacuolar strands seem to bisect the vacuole (Figure 2e); these represent cytoplasmic tunnels that traverse the lumen of the continuous vacuole and are permanently remodeled (Higaki *et al.*, 2006; Hoffmann and Nebenführ, 2004; Ruthardt *et al.*, 2005). Transvacuolar strands are delimited by the tonoplast and can contain all other cytoplasmic organelles, with the exception of the

nucleus. Some cells, particularly in rapidly expanding tissues of seedlings, contain circular structures of varying size (1–10 μm) inside the lumen of the vacuole (Figure 2d). These structures are sometimes referred to as 'bulbs', and are invaginations of the tonoplast membrane that are continuous with the outer vacuolar membrane (Saito *et al.*, 2002). The number of bulbs per cell appears to correlate with the expression level of the marker, although they are also found in untransformed cells (Saito *et al.*, 2002).

The tonoplast is almost invisible when viewed in a focal plane close to the plasma membrane because the fluorescence signal is more or less uniform across the field of view (not shown). However, it can be visualized easily in cross section, i.e. when focusing near the center of the cell. In this focal plane, the ER may be mistaken for the tonoplast because of their largely similar distribution and the thinness of the cytoplasm in fully expanded cells (Figure 2, compare g and h). However, the fluorescence signal of the tonoplast marker is very uniform in both intensity and thickness. In contrast, the ER signal is often patterned and of variable thickness, reflecting the distance of the tonoplast from the plasma membrane. Another distinctive feature that allows the discrimination of these two organelles is their distribution around the nucleus. The tonoplast approaches the nucleus only on the side facing the interior of the cell, whereas the ER is also found between the nucleus and the plasma membrane (Figure 2, compare c and f).

The plasma membrane surrounds the cytoplasm on all sides as a single layer. Hence, proteins that localize to this membrane display uniform labeling along the surface of the cell (Figure 2k), which is similar to the tonoplast (Figure 2h) but different from the patterned labeling seen for ER-localized proteins (Figure 2g). Unlike the tonoplast (or the ER), however, the plasma membrane does not enter the interior of the cell, and is not found in transvacuolar strands or on the side of the nucleus facing the vacuole. The plasma membrane marker can also be used to define the area of the cell wall by identifying the surfaces of two neighboring cells (not shown).

Application example: localization of uncharacterized proteins

The organelle markers presented here can be used to localize uncharacterized proteins. To illustrate this process we have chosen three *Arabidopsis* genes, the products of which have not previously been examined cytologically for their intracellular distribution. Some of the proteins were selected based on their predicted targeting signals, whereas others were selected because their annotated location was contradicted by organelle-specific proteomics. For all candidates, intracellular localization was predicted by several web-based algorithms (for details, see Experimental procedures). Coding regions of the genes were amplified from cDNA and fused at the N-terminus of YFP, as none of the proteins contained any known C-terminal targeting signals. Plasmids containing expression cassettes of the YFP fusions were bombarded into *Arabidopsis* leaf epidermal cells of CFP organelle marker lines, or were co-bombarded with CFP-based markers. In Figure 3 the CFP organelle marker is false-colored magenta, whereas the candidate YFP signal is false-colored green.

The At1g22590 gene is annotated as encoding a putative MADS box protein, which suggests a putative function as a transcription factor in the nucleus (Kramer and Hall, 2005). However, several computer programs predicted import of this protein into mitochondria (Table 2). Only PSORT gave equal probability of mitochondrial and nuclear targeting (Table 2). The At1g22590-YFP fusion protein was localized predominantly in a large, round area (Figure 3a); however, weak diffuse YFP fluorescence was also detected throughout the cytoplasm. None of the organelle markers in this set matched this distribution; most notably the mitochondrial marker gave a very different labeling pattern (Figure 3a). The size of the YFP-labeled spot is consistent with it being the nucleus. This interpretation was indirectly supported by comparison with the ER-CFP marker, which surrounded the At1g22590-YFP fluorescence on all sides (Figure 3b). Thus, the co-localization experiment corroborated the annotation

Table 2 Prediction of intracellular localization of candidate proteins

AGI	At1g22590	At3g15000	At5g19750
Annotation	MADS-box	DAG-like	Peroxisomal 22-kDa family
Proteomics	–	Mitochondria	Chloroplast
TargetP	n.p.	Chloroplast	Chloroplast
Predotar	Mitochondria	Plastid/mitochondria	Mitochondria
MitoProt	$P = 0.6$	$P = 0.99$	$P = 0.79$
WolfPSORT	Mitochondria (8), chloroplast (4), nucleus (2)	Chloroplast (7), mitochondria (6), nucleus (1)	Chloroplast (4), nucleus (4), ER (4)
PSORT	Nucleus (0.60), mitochondria (0.58)	Chloroplast (0.90), mitochondria (0.76)	PM (0.60), chloroplast (0.50), Golgi (0.40)
iPSORT	Signal peptide	Chloroplast	Chloroplast

n.p., no prediction; ER, endoplasmic reticulum.

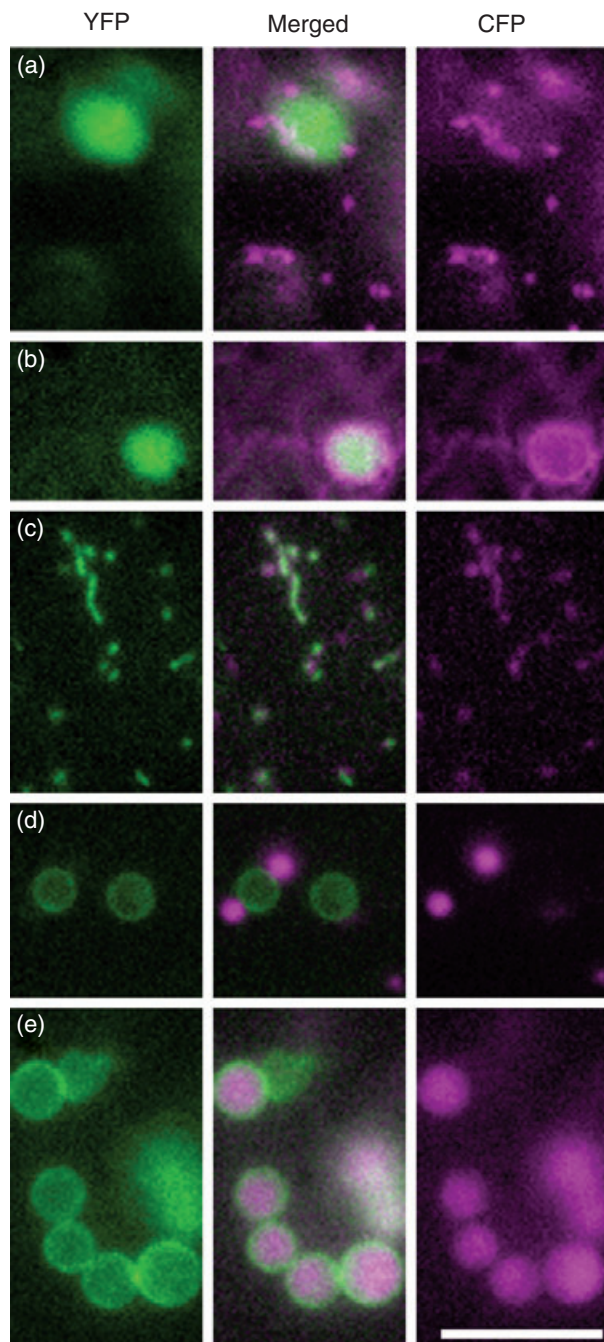


Figure 3. Co-localization of uncharacterized proteins with organelle markers. YFP fusions to the uncharacterized proteins are shown in green; CFP organelle markers are shown in magenta.

- (a) At1g22590-YFP was present in a large bright spot that did not co-localize with mitochondria.
 (b) The bright At1g22590-YFP label was completely surrounded by the endoplasmic reticulum (ER) marker, suggesting that this spot corresponds to the nucleus.
 (c) At3g15000-YFP co-localized with the mitochondrial marker. Pairs of green and magenta spots resulted from movement of these mitochondria between image captures.
 (d) The putative peroxisomal membrane protein At5g19750-YFP formed large rings that did not coincide with peroxisomes.
 (e) At5g19750-YFP rings labeled the surface of chloroplasts in a guard cell. Scale bar = 10 μ m.

of At1g22590 as a putative transcription factor, and contradicted most bioinformatic predictions.

The At3g15000 gene is annotated as similar to the *DAG* (*differentiation and greening*) gene from *Antirrhinum majus*, which is necessary for chloroplast differentiation as well as palisade development (Chatterjee *et al.*, 1996). The prediction algorithms gave nearly equal probability for chloroplast and mitochondrial localization (Table 2). Interestingly, the At3g15000 protein was isolated with the mitochondrial proteome of suspension cell cultures (Heazlewood *et al.*, 2004). The At3g15000-YFP fusion protein was co-localized exclusively with the mitochondria-CFP marker (Figure 3c), confirming the proteomic data. However, we cannot formally exclude the possibility that At3g15000 could also be imported into chloroplasts in green tissues because we have only observed epidermal cells.

The last candidate tested, At5g19750, is annotated as a member of the 22-kDa peroxisomal membrane protein gene family. Most of the prediction programs used in this study are not able to identify peroxisomal targeting sequences, and instead return a wide range of different localizations. Even PSORT, the only program specifically able to predict peroxisomal targeting, gave the secretory pathway as the likely localization. Curiously, the At5g19750 protein was identified as part of the chloroplast proteome (Ferro *et al.*, 2002). Comparison of At5g19750-YFP labeling with the peroxisome-CFP marker did not reveal any co-localized signals (Figure 3d). Instead, the fusion protein labeled larger structures reminiscent of plastids. Expression of At5g19750-YFP in the plastid-CFP marker lines demonstrated limited co-localization, with the YFP signal forming a thin border surrounding the CFP-labeled stroma (Figure 3e). This pattern is suggestive of localization of At5g19750-YFP to the plastid envelope (inner or outer membrane). Thus, the experimentally determined localization is consistent with the proteomic data and contradicts the gene annotation.

In summary, the organelle markers lines have allowed us to quickly determine the subcellular localization of previously uncharacterized proteins. This experimental evidence of organelle targeting sometimes contradicted the computational predictions from various algorithms. These discrepancies should not come as a surprise, as the output of the prediction programs is usually based on only partially defined targeting signals that allow a high degree of sequence variability. Unless targeting signals are defined more precisely, based on large-scale localization experiments similar to those described here, all prediction algorithms will suffer from a high level of misinterpretation. Furthermore, many of the prediction algorithms focus only on a subset of organelles (e.g. PredoTar for mitochondria and plastids; Small *et al.*, 2004) and are therefore not useful to analyze proteins that target to other compartments.

A more important conclusion from our brief survey is that the YFP-fusion approach, in combination with this organelle marker set, can be used to efficiently test unexpected results from organelle proteomics. Identification of unanticipated proteins within subcellular fractions could result either from spurious contamination or from incorrect assumptions. Localization studies such as those described here can provide an independent test of the proteomic data, and can thus be used to distinguish between these possibilities.

A limitation of the simple approach described here is that it relies on transient expression of FP fusions in epidermal tissues. A further concern must be that the fusion site on the candidate protein should not interfere with any targeting signals necessary for proper localization. This can be avoided by sequence comparison to established targeting sequences (e.g. <http://www.expasy.org/tools>), although not all possible targeting sequences are currently known. A good general approach may be to insert the FP moiety shortly before the C-terminus of the candidate protein, provided that this does not disrupt known protein domains (Tian *et al.*, 2004). Tissue-specific targeting of the markers to different organelles does not appear to be an issue. The organelles represented in this marker set appear to rely on targeting mechanisms that probably exist in all cell types. We have not observed any alternative labeling patterns in a wide variety of tissues of the transgenic lines for all marker constructs. In those rare situations where an uncharacterized protein appears to target differently depending on the cell type, the use of the native promoters of the candidate gene in combination with the organelle marker plants should reveal the correct intracellular localization.

Conclusions

We have generated a series of fluorescent organelle markers that can be used for co-localization studies with a wide range of other proteins. The markers themselves can also be used for visualizing organelle dynamics in living cells, which could be of interest for plant biology classes. The availability of the markers in two different binary plasmids gives additional flexibility for transforming any species of interest, either stably or transiently, e.g. by leaf infiltration (Batoko *et al.*, 2000). The complete organelle marker set is available through the Arabidopsis stock centers (<http://www.arabidopsis.org>) and is also described on our web site (<http://www.bio.utk.edu/cellbiol/markers>).

Experimental procedures

Generation of organelle marker lines

All organelle markers were first assembled and tested in pBluescript (Stratagene, <http://www.stratagene.com>) based expression vectors

that contained GFP, CFP, YFP or mCherry, respectively, flanked by a double 35S promoter and the nopaline synthase (*nos*) 3' polyA signal (AN, unpublished data). Plastid markers were created by amplification of the targeting signal from tobacco rubisco small subunit cDNA (a kind gift of Dr Bruce, University of Tennessee; Dabney-Smith *et al.*, 1999) with the primers 5'-CGAGCTAGCATGGCTTCCTCAGTCTTTC and 5'-GCAGGATCCGCTCAAATCAGGAAGGTATGA and insertion in front of the FP after digestion with *NheI* and *Bam*HI (restriction sites are underlined in the primer sequences). The mitochondrial targeting signal of yeast *ScCOX4* (Köhler *et al.*, 1997) was amplified from genomic DNA (a kind gift of Dr Masi, University of Tennessee) with the primers 5'-CGATCTAGAATGCTTTCACCTACGTAATCTATAA and 5'-GCA-GGATCCGGGTTTTGCTGAAGCAGATATC and ligated in front of the FP gene after *XbaI/Bam*HI digest. Peroxisomal markers are based on published vectors similar to ours (von Arnim *et al.*, 1998), but with an additional tobacco mosaic virus (TMV) translational enhancer element in front of the FP coding region. The PTS1 sequence was encoded on a synthetic oligonucleotide (5'-GATCGAAGCTGTAAGATCTAGA) and inserted in frame at the C-terminus of the FPs after *Bgl*II/*XbaI* digest. The Golgi marker has been described previously as Man49-GFP (Saint-Jore-Dupas *et al.*, 2006). The ER marker was created by first inserting a synthetic oligonucleotide encoding HDEL (5'-AGATCTCATGACGAGCTGTAAGTGCAGTCTAGA) at the C-terminus of the FP genes and subsequently adding the signal peptide of AtWAK2 (He *et al.*, 1999) at the N-terminus. Amplification of the signal peptide from a cDNA (a kind gift of Dr Kohorn, Duke University) was achieved with primers 5'-CGATCTAGAGAGAAGATGAAGGTACAGGAG and 5'-GCA-GATCCGCACTCCTTGCGAGGTTGC. The GFP tonoplast marker was a kind gift of Dr Nakano (RIKEN) and was first described by Saito *et al.* (2002). To create the other FP versions, the γ -TIP coding region was excised from the original plasmid with *XbaI/Bam*HI digest and ligated into expression vectors encoding CFP, YFP or mCherry, respectively. The plasma membrane marker is based on a full-length fusion of the aquaporin PIP2A to FPs. PIP2A cDNA (GenBank accession X75883.1) was amplified from leaf cDNA using the primers 5'-ACGTCTAGAATGGCAAAGGATGTGGAAGC and 5'-GCA-GGATCCGCACTCCTTGCGAGGTTGC and inserted in front of the FP coding region after *XbaI/Bam*HI digest.

All marker plasmids were confirmed by sequencing and were tested by particle bombardment into onion epidermal peels. The expression cassettes were then moved with conventional restriction digestion followed by DNA ligation into two different binary plasmids, pBIN20 (Hennegan and Danna, 1998) and a pFGC5941 derivative (Kerschen *et al.*, 2004), respectively. Transgenic *A. thaliana* lines (Col) were created with the pBIN-based binary plasmids by the floral-dip method (Clough and Bent, 1998) and selected with kanamycin.

Bioinformatic analysis

At1g22590 was chosen for its predicted localization to mitochondria. At3g15000 and At5g19750 were chosen from the SUBA database (<http://www.suba.bcs.uwa.edu.au>; Heazlewood *et al.*, 2005) from a list of proteins that were not previously localized by fluorescence microscopy. For the proteins selected, annotations of protein function were obtained from SUBA and/or the gene locus information from TAIR (<http://www.arabidopsis.org>).

Several programs were used to predict subcellular localization and to identify potential targeting regions that could be disrupted by the translational fusion to YFP. These programs can be accessed at the ExpASY website (<http://www.expasy.org>). Programs used to predict subcellular localization were WolfPSORT (Horton *et al.*,

2006), PSORT (Nakai and Kanehisa, 1991), iPSORT (Bannai et al., 2002), TargetP.1 (Emanuelsson et al., 2000), MitoProt II (Claros and Vicens, 1996) and Predotar (Small et al., 2004). Programs for the identification of known domains and transmembrane regions were TMHMM (Sonnhammer et al., 1998), TMPred (Hofman and Stoffel, 1993), SOSUI (Hirokawa et al., 1998; Mitaku et al., 2002) and TopPred (Claros and von Heijne, 1994).

Translational fusions of uncharacterized proteins

RNA was purified from *A. thaliana* leaves and flowers, and was amplified by reverse transcriptase PCR (RT-PCR). At1g22590 was amplified from flower cDNA with the primers 5'-CGAGCTAGCATGGGAAGAAGAAAAGTTAC and 5'-GCAGACGTCGCTCTCTTGTGATTGGTGC. At3g15000 and At5g19750 were amplified from leaf cDNA with the primers 5'-CGAGCTAGCATGGCGACCATACC and 5'-GCAGGATCCACCCTGGTAGGGTT or 5'-CGAGCTAGCATGCTTAACTCTATC and 5'-GCAGGATCCCTTGCACAACTTC, respectively. Once amplified, At1g22590 was digested with *AatII* and *BamHI*, and At3g15000 and At5g19750 were digested with *NheI* and *BamHI* and were inserted between a double 35S promoter and the YFP coding region of a pBluescript-based expression vector (pAN95; unpublished data, A. Nebenführ). As the C-terminus of the encoded proteins did not contain a predicted transmembrane domain or a predicted targeting sequence, we did not expect any changes in protein localization to result from these C-terminal fusions. All insertions were confirmed by DNA sequencing.

Particle bombardment

Plasmids containing the genes encoding the uncharacterized proteins and/or the organelle markers were bombarded into 10-day-old Arabidopsis seedlings, young (1-cm long) leaves of 3-week-old Arabidopsis or onion epidermal peels following the manufacturer's recommendations. Briefly, between 100 ng and 1 µg of plasmid DNA was coated on 25 µl of 60 mg ml⁻¹ tungsten particles (Bio-Rad M10, 0.7 µm; Bio-Rad, <http://www.bio-rad.com>) in the presence of 1 M MgCl₂ and 15 mM spermidine for at least 5 min on a vortex mixer. Plasmid-coated particles were dehydrated with several ethanol washes and allowed to dry on plastic discs. Particles were accelerated with a helium burst at 1100 psi in a PDS-1000/He instrument (Bio-Rad). Seedlings (on half-strength MS plates) were returned to the growth chamber and detached leaves were kept in a moist chamber in the dark. For onion epidermal peels, the same procedure was followed except that 1-µm tungsten particles (Bio-Rad M17) were used and the peels were kept on half-strength MS plates overnight in the dark.

Microscopy

On the following day (16–24 h after bombardment), the localization of the expressed proteins was visualized with an Axiovert 200 M microscope (Zeiss, <http://www.zeiss.com>) equipped with filters for YFP and CFP fluorescence (filter set 52017; Chroma, <http://www.chroma.com>). Transformed cells were first identified under a 20× objective before representative cells were observed with a 63× (1.4 NA) plan-apo oil immersion objective. Images were captured with a digital camera (Orca ER; Hamamatsu Photonics, <http://www.hamamatsu.com>) controlled by OPENLAB software (Improvision, <http://www.improvision.com>). After background subtraction to remove camera noise, contrast enhancement was performed to increase signal intensity and remove low-level background fluorescence. For co-localization

experiments, YFP signals were false-colored green and CFP signals were false-colored magenta (red + blue). Photographs were subsequently processed for optimal presentation with PHOTOSHOP 7.0 (Adobe, <http://www.adobe.com>).

Acknowledgements

We thank Dr Barry Bruce (University of Tennessee), Dr Bruce Kohorn (Duke University), Dr Tom Masi (University of Tennessee), Dr Akihiho Nakano (RIKEN) and Eric Vincill (University of Tennessee) for DNA samples that allowed us to construct the organelle markers. We acknowledge the assistance of Kevin Allen, Prakitchai Chotewutmontri, Star N. Loar and Eunsook Park in the assembly of some of the fluorescent marker plasmids. Research in the Nebenführ lab is supported by the National Science Foundation, grant MCB-0416931 to AN.

References

- von Arnim, A.G., Deng, X.-W. and Stacey, M.G. (1998) Cloning vectors for the expression of green fluorescent protein fusion proteins in transgenic plants. *Gene*, **221**, 35–43.
- Baldwin, T.C., Handford, M.G., Yuseff, M.-I., Orellana, A. and Dupree, P. (2001) Identification and characterization of GONST1, a Golgi-localized GDP-mannose transporter in Arabidopsis. *Plant Cell*, **13**, 2283–2295.
- Bannai, H., Tamada, Y., Maruyama, O., Nakai, K. and Miyano, S. (2002) Extensive feature detection of N-terminal protein sorting signals. *Bioinformatics*, **18**, 298–305.
- Batoko, H., Zheng, H.-Q., Hawes, C. and Moore, I. (2000) A Rab1 GTPase is required for transport between the endoplasmic reticulum and Golgi apparatus and for normal Golgi movement in plants. *Plant Cell*, **12**, 2201–2218.
- Boevink, P., Oparka, K., Sant Cruz, S., Martin, B., Betteridge, A. and Hawes, C. (1998) Stacks on tracks: the plant Golgi apparatus traffics on an actin/ER network. *Plant J.* **15**, 441–447.
- Brandizzi, F., Snapp, E., Roberts, A., Lippincott-Schwartz, J. and Hawes, C. (2002) Membrane protein transport between the ER and Golgi in tobacco leaves is energy dependent but cytoskeleton independent: evidence from selective photobleaching. *Plant Cell*, **14**, 1293–1309.
- Chatterjee, M., Sparvoli, S., Edmunds, C., Garosi, P., Findlay, K. and Martin, C. (1996) DAG, a gene required for chloroplast differentiation and palisade development in *Antirrhinum majus*. *EMBO J.* **15**, 4194–4207.
- Claros, M.G. and Vicens, P. (1996) Computational method to predict mitochondrially imported proteins and their targeting sequences. *Eur. J. Biochem.* **241**, 779–786.
- Claros, M.G. and von Heijne, G. (1994) TopPred II: an improved software for membrane protein structure predictions. *CABIOS*, **10**, 685–686.
- Clough, S.J. and Bent, A.F. (1998) Floral dip: a simplified method for *Agrobacterium*-mediated transformation of *Arabidopsis thaliana*. *Plant J.* **16**, 735–743.
- Collings, D.A., Carter, C.N., Rink, J.C., Scott, A.C., Wyatt, S.E. and Allen, N.S. (2000) Plant nuclei can contain extensive grooves and invaginations. *Plant Cell*, **12**, 2425–2440.
- Collings, D.A., Harper, J.D.I., Marc, J., Overall, R.L. and Mullen, R.T. (2002) Life in the fast lane: actin-based motility of plant peroxisomes. *Can. J. Bot.* **80**, 430–441.
- Crofts, A.J., Leborgne-Castel, N., Hillmer, S., Robinson, D.G., Phillipson, B., Carlsson, L.E., Ashford, D.A. and Denecke, J. (1999)

- Saturation of the endoplasmic reticulum retention machinery reveals anterograde bulk flow. *Plant Cell*, **11**, 2233–2247.
- Cutler, S.R., Ehrhardt, D.W., Griffiths, J.S. and Somerville, C.R.** (2000) Random GFP::cDNA fusions enable visualization of subcellular structures in cells of *Arabidopsis* at a high frequency. *Proc. Natl Acad. Sci. USA*, **97**, 3718–3723.
- Dabney-Smith, C., van den Wijngaard, P.W.J., Treece, Y., Vredenberg, W.J. and Bruce, B.D.** (1999) The C terminus of a chloroplast precursor modulates its interaction with the translocation apparatus and PIRAC. *J. Biol. Chem.* **274**, 32351–32359.
- Dhanoo, P.K., Sinclair, A.M., Mullen, R.T. and Mathur, J.** (2006) Illuminating subcellular structures and dynamics in plants: a fluorescent protein toolbox. *Can. J. Bot.* **84**, 515–522.
- Dixit, R., Cyr, R. and Gilroy, S.** (2006) Using intrinsically fluorescent proteins for plant cell imaging. *Plant J.* **45**, 599–615.
- Dunkley, T.P.J., Hester, S., Shadforth, I.P. et al.** (2006) Mapping the *Arabidopsis* organelle proteome. *Proc. Natl Acad. Sci. USA*, **103**, 6518–6523.
- Emanuelsson, O. and von Heijne, G.** (2001) Prediction of organellar targeting signals. *Biochim. Biophys. Acta*, **1541**, 114–119.
- Emanuelsson, O., Nielsen, H., Brunak, S. and von Heijne, G.** (2000) Predicting subcellular localization of proteins based on their N-terminal amino acid sequence. *J. Mol. Biol.* **300**, 1005.
- Escobar, N.M., Haupt, S., Thow, G., Boevink, P., Chapman, S. and Oparka, K.** (2003) High-throughput viral expression of cDNA–green fluorescent protein fusions reveals novel subcellular addresses and identifies unique proteins that interact with plasmodesmata. *Plant Cell*, **15**, 1507–1523.
- Ferro, M., Salvi, D., Rivière-Rolland, H., Vermat, T., Seigneurin-Berny, D., Grunwald, D., Garin, J., Joyard, J. and Rolland, N.** (2002) Integral membrane proteins of the chloroplast envelope: identification and subcellular localization of new transporters. *Proc. Natl Acad. Sci. USA*, **99**, 11487–11492.
- van Gestel, K., Köhler, R.H. and Verbelen, J.-P.** (2002) Plant mitochondria move on F-actin, but their positioning in the cortical cytoplasm depends on both F-actin and microtubules. *J. Exp. Bot.*, **53**, 659–667.
- Gomord, V., Denmat, L.-A., Fichette-Lainé, A.-C., Satiat-Jeunemaitre, B., Hawes, C. and Faye, L.** (1997) The C-terminal HDEL sequence is sufficient for retention of secretory proteins in the endoplasmic reticulum (ER) but promotes vacuolar targeting of proteins that escape the ER. *Plant J.* **11**, 313–325.
- Hawes, C., Saint-Jore, C., Martin, B. and Zheng, H.-Q.** (2001) ER confirmed as the location of mystery organelles in *Arabidopsis* plants expressing GFP. *Trends Plant Sci.* **6**, 245–246.
- He, Z.-H., Cheeseman, I., He, D. and Kohorn, B.D.** (1999) A cluster of five cell wall-associated receptor kinase genes, Wak1–5, are expressed in specific organs of *Arabidopsis*. *Plant Mol. Biol.* **39**, 1189–1196.
- Heazlewood, J.L., Tonti-Filippini, J.S., Gout, A.M., Day, D.A., Whelan, J. and Millar, A.H.** (2004) Experimental analysis of the *Arabidopsis* mitochondrial proteome highlights signaling and regulatory components, provides assessment of targeting prediction programs, and indicates plant-specific mitochondrial proteins. *Plant Cell*, **16**, 241–256.
- Heazlewood, J.L., Tonti-Filippini, J., Verboom, R.E. and Millar, A.H.** (2005) Combining experimental and predicted datasets for determination of the subcellular location of proteins in *Arabidopsis*. *Plant Physiol.* **139**, 598–609.
- Hennegan, K.P. and Danna, K.J.** (1998) pBIN20: an improved binary vector for *Agrobacterium*-mediated transformation. *Plant Mol. Biol. Rep.* **16**, 129–131.
- Higaki, T., Kutsuna, N., Okubo, E., Sano, T. and Hasezawa, S.** (2006) Actin microfilaments regulate vacuolar structures and dynamics: dual observation of actin microfilaments and vacuolar membrane in living tobacco BY-2 cells. *Plant Cell Physiol.* **47**, 839–852.
- Hirokawa, T., Boon-Chieng, S. and Mitaku, S.** (1998) SOSUI: classification and secondary structure prediction system for membrane proteins. *Bioinformatics*, **14**, 378–379.
- Hoffmann, A. and Nebenführ, A.** (2004) Dynamic rearrangements of transvacuolar strands in BY-2 cells imply a role of myosin in remodeling the plant actin cytoskeleton. *Protoplasma*, **224**, 201–210.
- Hofman, K. and Stoffel, W.** (1993) TMbase - A database of membrane spanning proteins segments. *Biol. Chem.* **374**, 166.
- Horton, P., Park, K.-J., Obayashi, T. and Nakai, K.** (2006) *Protein Subcellular Localization Prediction with WoLF PSORT*. 4th Annual Asia Pacific Bioinformatics Conference APBC06, Taipei, Taiwan. London: Imperial College Press, pp. 39–48.
- Jauh, G.-Y., Phillips, T.E. and Rogers, J.C.** (1999) Tonoplast intrinsic protein isoforms as markers for vacuolar functions. *Plant Cell*, **11**, 1867–1882.
- Jedd, G. and Chua, N.-H.** (2002) Visualization of peroxisomes in living plant cells reveals actomyosin dependent cytoplasmic streaming and peroxisome budding. *Plant Cell Physiol.* **43**, 384–392.
- Kerschen, A., Napoli, C.A., Jorgensen, R.A. and Müller, A.E.** (2004) Effectiveness of RNA interference in transgenic plants. *FEBS Lett.* **566**, 223–228.
- Köhler, R.H., Zipfel, W.R., Webb, W.W. and Hanson, M.R.** (1997) The green fluorescent protein as a marker to visualize plant mitochondria *in vivo*. *Plant J.* **11**, 613–621.
- Komatsu, S., Konishi, H. and Hashimoto, M.** (2006) The proteomics of plant cell membranes. *J. Exp. Bot.* **58**, 103–112.
- Koroleva, O.A., Tomlinson, M.L., Leader, D., Shaw, P. and Doonan, J.H.** (2005) High-throughput protein localization in *Arabidopsis* using *Agrobacterium*-mediated transient expression of GFP-ORF fusions. *Plant J.* **41**, 162–174.
- Kramer, E.M. and Hall, J.C.** (2005) Evolutionary dynamics of genes controlling floral development. *Curr. Opin. Plant Biol.* **8**, 13–18.
- Kwok, E.Y. and Hanson, M.R.** (2003) Microfilaments and microtubules control the morphology and movement of non-green plastids and stromules in *Nicotiana tabacum*. *Plant J.* **35**, 16–26.
- Kwok, E.Y. and Hanson, M.R.** (2004) *In vivo* analysis of interactions between GFP-labeled microfilaments and plastid stromules. *BMC Plant Biol.* **4**, 2.
- Li, S., Ehrhardt, D.W. and Rhee, S.Y.** (2006) Systematic analysis of *Arabidopsis* organelles and a protein localization database for facilitating fluorescent tagging of full-length *Arabidopsis* proteins. *Plant Physiol.* **141**, 527–539.
- Lilley, K.S. and Dupree, P.** (2006) Methods of quantitative proteomics and their application to plant organelle characterization. *J. Exp. Bot.* **57**, 11493–11499.
- Logan, D.C.** (2006) Plant mitochondrial dynamics. *Biochim. Biophys. Acta*, **1763**, 430–441.
- Lunn, J.E.** (2006) Compartmentation in plant metabolism. *J. Exp. Bot.* **58**, 35–47.
- Mano, S., Nakamori, C., Hayashi, M., Kato, A., Kondo, M. and Nishimura, M.** (2002) Distribution and characterization of peroxisomes in *Arabidopsis* by visualization with GFP: dynamic morphology and actin-dependent movement. *Plant Cell Physiol.* **43**, 331–341.
- Mathur, J., Mathur, N. and Hülskamp, M.** (2002) Simultaneous visualization of peroxisomes and cytoskeletal elements reveals actin and not microtubule-based peroxisome motility in plants. *Plant Physiol.* **128**, 1031–1045.
- Matsushima, R., Kondo, M., Nishimura, M. and Hara-Nishimura, I.** (2003) A novel ER-derived compartment, the ER body, selectively

- accumulates a β -glucosidase with an ER-retention signal in *Arabidopsis*. *Plant J.* **33**, 493–502.
- Mitaku, S., Hirokawa, T. and Tsuji, T.** (2002) Amphiphilicity index of polar amino acids as an aid in the characterization of amino acid preference at membrane-water interfaces. *Bioinformatics*, **18**, 608–616.
- Molendijk, A.J., Ruperti, B. and Palme, K.** (2004) Small GTPases in vesicle trafficking. *Curr. Opin. Plant Biol.* **7**, 694–700.
- Muench, D.G. and Mullen, R.T.** (2003) Peroxisome dynamics in plant cells: a role for the cytoskeleton. *Plant Sci.* **164**, 307–315.
- Nakai, K. and Kanehisa, M.** (1991) Expert system for predicting localization sites in gram-negative bacteria. *Proteins*, **11**, 95–110.
- Nebenführ, A., Gallagher, L., Dunahay, T.G., Frohlick, J.A., Masurkiewicz, A.M., Meehl, J.B. and Staehelin, L.A.** (1999) Stop-and-go movements of plant Golgi stacks are mediated by the actomyosin system. *Plant Physiol.* **121**, 1127–1141.
- Nebenführ, A., Ritzenthaler, C. and Robinson, D.G.** (2002) Brefeldin A: deciphering an enigmatic inhibitor of secretion. *Plant Physiol.* **130**, 1102–1108.
- Oikawa, K., Kasahara, M., Kiyosue, T., Kagawa, T., Suetsugu, N., Takahashi, F., Kanegae, T., Niwa, Y., Kadota, A. and Wada, M.** (2003) CHLOROPLAST UNUSUAL POSITIONING1 is essential for proper chloroplast positioning. *Plant Cell*, **15**, 2805–2815.
- Reumann, S.** (2004) Specification of the peroxisome targeting signals type 1 and type 2 of plant peroxisomes by bioinformatic analysis. *Plant Physiol.* **135**, 763–800.
- Ritzenthaler, C., Nebenführ, A., Movafeghi, A., Stussi-Garaud, C., Behnia, L., Pimpl, P., Staehelin, L.A. and Robinson, D.G.** (2002) Reevaluation of the effects of brefeldin A on plant cells using tobacco bright yellow 2 cells expressing Golgi-targeted green fluorescent protein and COPI antisera. *Plant Cell*, **14**, 237–261.
- Runions, J., Brach, T., Kühner, S. and Hawes, C.** (2006) Photoactivation of GFP reveals protein dynamics within the endoplasmic reticulum membrane. *J. Exp. Bot.* **57**, 43–50.
- Ruthardt, N., Gulde, N., Spiegel, H., Fischer, R. and Emans, N.** (2005) Four-dimensional imaging of transvacuolar strand dynamics in tobacco BY-2 cells. *Protoplasma*, **225**, 205–215.
- Saint-Jore, C.M., Evins, J., Batoko, H., Brandizzi, F., Moore, I. and Hawes, C.** (2002) Redistribution of membrane proteins between the Golgi apparatus and endoplasmic reticulum in plants is reversible and not dependent on cytoskeletal networks. *Plant J.* **29**, 661–678.
- Saint-Jore-Dupas, C., Nebenführ, A., Boulaflois, A., Follet-Gueye, M.-L., Plasson, C., Hawes, C., Driouich, A., Faye, L. and Gornod, V.** (2006) Plant N-glycan processing enzymes employ different targeting mechanisms for their spatial arrangement along the secretory pathway. *Plant Cell*, **18**, 3182–3200.
- Saito, C., Ueda, T., Abe, H., Wada, Y., Kuroiwa, T., Hisada, A., Furuya, M. and Nakano, A.** (2002) A complex and mobile structure forms a distinct subregion within the continuous vacuolar membrane in young cotyledons of *Arabidopsis*. *Plant J.* **29**, 245–255.
- Satiat-Jeuemaitre, B., Cole, L., Bouret, T., Howard, R. and Hawes, C.** (1996) Brefeldin A effects in plant and fungal cells: something new about vesicle trafficking? *J. Microsc.* **181**, 162–177.
- Shaner, N.C., Campbell, R.E., Steinbach, P.A., Giepmans, B.N.G., Palmer, A.E. and Tsien, R.Y.** (2004) Improved monomeric red, orange and yellow fluorescent proteins derived from *Discosoma* sp. red fluorescent protein. *Nat. Biotechnol.* **22**, 1567–1572.
- Shaw, S.L.** (2006) Imaging the live plant cell. *Plant J.* **45**, 573–588.
- Small, I., Peeters, N., Legeai, F. and Lurin, C.** (2004) Predotar: a tool for rapidly screening proteomes for N-terminal targeting sequences. *Proteomics*, **4**, 1581–1590.
- Sonnhammer, E.L.L., von Heijne, G. and Krogh, A.** (1998) Hidden Markov model for predicting transmembrane helices in protein sequences. Proceedings of Sixth International Conference on Intelligent Systems for Molecular Biology, Menlo Park, CA: AAAI Press.
- Tamura, K., Shimada, T., Ono, E., Tanaka, Y., Nagatani, A., Higashi, S.-I., Watanabe, M., Nishimura, M. and Hara-Nishimura, I.** (2003) Why green fluorescent fusion proteins have not been observed in the vacuoles of higher plants. *Plant J.* **35**, 545–555.
- Tian, G.-W., Mohanty, A., Chary, S.N. et al.** (2004) High-throughput fluorescent tagging of full-length *Arabidopsis* gene products in planta. *Plant Physiol.* **135**, 25–38.
- Tse, Y.C., Mo, B., Hillmer, S., Zhao, M., Lo, S.W., Robinson, D.G. and Jiang, L.** (2004) Identification of multivesicular bodies as prevacuolar compartments in *Nicotiana tabacum* BY-2 cells. *Plant Cell*, **16**, 672–693.
- Uemura, T., Ueda, T., Ohniwa, R.L., Nakano, A., Takeyasu, K. and Sato, M.H.** (2004) Systematic analysis of SNARE molecules in *Arabidopsis*: dissection of the post-Golgi network in plant cells. *Cell Struct. Funct.* **29**, 49–65.
- Vitale, A. and Denecke, J.** (1999) The endoplasmic reticulum – gateway of the secretory pathway. *Plant Cell*, **11**, 615–628.
- Vitale, A. and Raikhel, N.V.** (1999) What do proteins need to reach different vacuoles? *Trends Plant Sci.* **4**, 149–155.
- Wee, E.G.-T., Sherrier, D.J., Prime, T.A. and Dupree, P.** (1998) Targeting of active sialyltransferase to the plant Golgi apparatus. *Plant Cell*, **10**, 1759–1768.

For accession numbers/seed stocks see Table 1.